Title

A proteoliposome-based system reveals how lipids control photosynthetic light harvesting

Journal

Journal of Biological Chemistry, 295(7)

ISSN

0021-9258

Authors

Tietz, Stefanie
Leuenberger, Michelle
Höhner, Ricarda
et al.

Publication Date

2020-02-01

DOI

10.1074/jbc.ra119.011707

Peer reviewed

JBC Papers in Press. Published on January 12, 2020 as Manuscript RA119.011707
The latest version is at http://www.jbc.org/cgi/doi/10.1074/jbc.RA119.011707

A proteoliposome-based system reveals how lipids control photosynthetic light harvesting

Stefanie Tietz[1,#], Michelle Leuenberger[2,3], Ricarda Höhner[1,##], Alice H. Olson[1], Graham R. Fleming[2,3], Helmut Kirchhoff[1,*]

[a], Institute of Biological Chemistry, Washington State University, PO Box 646340, Pullman, WA, 99164-6340, USA.
[b], Department of Chemistry, University of California, Berkeley, CA 94720;
[c], Molecular Biophysics and Integrated Bioimaging Division, Lawrence Berkeley National Laboratory, Berkeley, CA 94720;

Running title: Lipid-induced energy quenching

[#]Present address: Michigan State University-Department of Energy Plant Research Laboratory, Michigan State University, East Lansing, MI, 48824, USA
[##]Present address: School of Biological Sciences, Washington State University, PO Box 644236, Pullman, WA
[*]To whom correspondence should be addressed: Helmut Kirchhoff, Institute of Biological Chemistry, Washington State University, PO Box 646340, Pullman, WA, 99164-6340, USA. T: +1 509 335 3304, F: +1 509 335 7643, kirchhh@wsu.edu

Keywords: Thylakoid membrane, light harvesting complex, non-bilayer lipid, monogalactosyldiacylglycerol, lateral membrane pressure, non-photochemical quenching, proteoliposome, lipid-protein interaction, photosynthesis, energy transduction, photosystem

Abstract

Integral membrane proteins are exposed to a complex and dynamic lipid environment modulated by non-bilayer lipids that can influence protein functions by lipid-protein interactions. The non-bilayer lipid monogalactosyldiacylglycerol (MGDG) is the most abundant lipid in plant photosynthetic thylakoid membranes, but its impact on the functionality of energy-converting membrane protein complexes is unknown. Here, we optimized a detergent-based reconstitution protocol to developed a proteoliposome technique that incorporates the major light-harvesting complex II (LHCII) into compositionally well-defined large unilamellar lipid bilayer vesicles to study the impact of MGDG on light harvesting by LHCII. Using steady-state fluorescence spectroscopy, CD spectroscopy, and time-correlated single-photon counting, we found that both chlorophyll fluorescence quantum yields and fluorescence lifetimes clearly indicate that the presence of MGDG in lipid bilayers switches LHCII from a light-harvesting to a more energy-quenching mode that dissipates harvested light into heat. Is it hypothesized that in the *in vitro* system developed here, MGDG controls light harvesting of LHCII by modulating of the hydrostatic lateral membrane pressure profile in the lipid bilayer sensed by LHCII-bound peripheral pigments.

Introduction

Photosynthetic energy transformation starts with the harnessing of solar photons and the spatial transfer of the collected light energy to photochemically active reaction centers localized within photosystems (PS) to ignite electron transport. The processes of light harvesting and energy transfer are realized by specialized light-harvesting pigment protein complexes (LHC, 1). LHCs were tuned by evolution for an almost loss-free ultrafast electronic excitation energy transfer between protein-anchored pigments (1,2). Some LHCs are not only perfect light harvesters, but in addition have the remarkable built-in capacity to switch from a light-harvesting mode to an efficient energy quenching mode under light stress (3,4,5). This energy quenching mode (qE) is one of the most important photoprotective mechanisms in photosynthetic organisms ensuring survival and fitness in a highly dynamic environment (6). In plants and algae, LHCs fulfill their dual role as light-harvester and energy quencher as transmembrane integral protein complexes buried in the amphiphilic thylakoid membrane system. Excellent structural data for the major plant LHCII exists that makes it an interesting candidate to study light harvesting in thylakoid membranes (7,8). LHCII serves as the main light harvesting antenna for PSII and under some conditions for PSI. Detailed structural information combined with data from ultra-fast and steady state spectroscopy leads to an in-depth understanding of the functionality of the isolated LHCII and its dynamic switch between light-harvesting and qE (e.g. 9,10,11). In native membranes, however, LHCII is embedded in a lipid bilayer. A substantial gap in our knowledge base exists on how the lipid matrix in thylakoid membranes interacts with LHCII (and other proteins) and modulates light-harvesting. For non-photosynthetic membrane protein complexes, like mechanosensitive channels and membrane transporters, strong evidence exists that the composition and physicochemical properties of the lipid bilayer has significant impact on the conformation and functionality of these proteins (12-17). A concept that bridges physicochemical lipid bilayer properties with structural and functional alterations of membrane proteins is the lateral membrane pressure (LMP) hypothesis (12,18) also known as force-from-lipid principle (17). The so-called non-bilayer lipids play a

central role in the LMP hypothesis. In contrast to bilayer forming lipids that have an overall cylindrical shape, non-bilayer lipids adopt a conical shape because their hydrophilic head group is smaller than the hydrophobic fatty acid tail. According to the lipid shape-structure concept (19) isolated conical shaped non-bilayer lipids adopt non-lamellar structures like inverted hexagonal (HII) phases in aqueous environments (rods of aligned lipids with the smaller head groups facing to the center of the rod and the fatty acids moiety facing outwards). Many biomembranes contain a high percentage of non-bilayer lipids. Thylakoid membranes are dominated by the non-bilayer lipid monogalactosyldiacylglycerol (MGDG) that make up about half of the total lipids (20,21). The role of MGDG in photosynthetic energy transformation and its regulation is not established and remains elusive (21). Recently, it was shown that the presence of MGDG in the lipid matrix increases the structural stability of LHCII. This observation was interpreted as a consequence of modulation of LMP by this non-bilayer lipid (22). Non-bilayer lipids generate a higher lateral membrane pressure in the hydrocarbon region of the lipid bilayer because of their bulkier fatty acid part requiring more space (12,13,18,23). The higher membrane pressure in the hydrophobic membrane region is sensed by membrane proteins that can modulate their conformation and functionality (24). For photosynthetic thylakoid membranes, molecular dynamics simulation confirmed that the presence of MGDG leads to a significant increase of the physical pressure in the hydrophobic fatty acid part (25). In this study, the impact of the non-bilayer lipid MGDG for LHCII functionality was tested by reconstituting isolated trimeric LHCII, from spinach, into lipid liposomes with different mol% of MGDG leading to proteoliposomes. Proteoliposomes are a versatile tool for studying energy-transducing membrane proteins (26) and have frequently used in photosynthesis research (e.g. 27-32). Here, a detergent-based reconstitution protocol (26,32) was optimized, which generated LHCII-proteoliposomes with a very low protein density allowing specifically the study of lipid-protein interactions.

Results

LHCII proteoliposomes with low protein density. Most studies on LHCII proteoliposomes used relatively high protein to lipid ratios leading to LHCII aggregation. LHCII aggregation is known to cause energy quenching by changes of the conformation of the pigment-protein complex (e.g. 33,34,35). LHCII aggregation interferes with lipid-only induced alterations of the LHCII structure and function. To avoid protein-protein interactions by LHCII aggregation, we refined a detergent-based reconstitution protocol leading to very low protein densities in the final LHCII-proteoliposomes (Fig. 1). Addition of detergent to preformed large unilamellar lipid vesicles (LUV, made of isolate thylakoid lipids) destabilize the LUV-bilayer necessary to allow LHCII-incorporation (step II in Fig. 1A). LHCII was isolated from spinach. We used the detergent Triton X-100 for the LUV-destabilization since it has a distinct absorption peak around 275 nm (Fig. 1A, bottom) that is missing for other detergents. The 275 nm Triton X-100 absorption peak is used to monitor detergent removal upon Bio bead treatment (Fig. 1A, bottom). Thus, it is ensured that the final LHCII-proteoliposomes are detergent free. The successful incorporation of LHCII into the liposomes is validated by co-localization of fluorescent dyes (SI Fig. 1) that stain the lumen of the proteoliposomes (pyranine), the lipid bilayer (BODIPY) and LHCII (chlorophyll auto-fluorescence). The final proteoliposomes have a mean diameter of

about 200 nm (Fig. 1B) determined by dynamic light scattering and a molar lipid to trimeric LHCII ratio of about 60,000 (Fig. 1C). Assuming that lipids are organized in a bilayer, occupy on average a molecular area of 0.66 nm^2 (36), and assuming that each LHCII-trimer binds 42 Chl (7,8) it follows that each proteoliposomes contains on average six LHCII trimers. This translates to a protein area fraction of smaller than 0.2% (area of trimeric LHCII is 33.2 nm^2), i.e. the LHCII concentration in proteoliposomes is very diluted. Two types of proteoliposomes were prepared to study the impact of MGDG on the LHCII functionality. One type contains MGDG and the other type contains almost no MGDG (small traces come as contamination from other thylakoid lipids). For the latter, MGDG was replaced by the charge-neutral DGDG. The lipid and fatty acid analysis measured for the final LHCII-proteoliposomes preparation is given in Fig. 1D. The fatty acid profile for the four thylakoid lipid classes is in accordance with the literature (37). Native thylakoid membranes contain about 50 mol% MGDG (20,21). We decided to produce proteoliposomes with no more than 25 mol% MGDG (Fig. 1D) since some reports mentioned that higher MGDG abundances in liposomes can lead to HII formation (22,38). Although it is debated whether high MGDG concentration leads to HII phase in liposomes we want to avoid non-bilayer HII formation in LHCII-proteoliposomes, and as a consequence the MGDG concentration was reduced to a "safe" value.

Structural integrity of LHCII in proteoliposomes. The structural integrity and protein aggregation level of LHCII in proteoliposomes was probed by fluorescence spectroscopy and circular dichroism (CD). Room temperature chlorophyll (chl) fluorescence spectra preferentially exciting chl a at 420 nm or chl b at 475 nm (39) reveal similar values for the maximal fluorescence emission wavelengths (SI Figs. 2A and 2B). This indicates efficient energy transfer from chl b to chl a in LHCII-proteoliposomes. This is further supported by almost indistinguishable normalized chl fluorescence emission spectra if exited at 420 nm or 475 nm for both MGDG-containing and -depleted proteoliposomes (SI Figs. 2C and 2D). The presence of excitonically disconnected chl b would lead to a blue-shifted shoulder for 475 nm excitation compared to 420 nm excitation. The lack of this shoulder gives clear evidence that all chl b is energetically well connected to the LHCII pigment system. Low temperature (77 K) fluorescence spectra (Fig. 2A) provides information about the unbinding of chls and LHCII aggregation. Diagnostic for chl b unbinding is an emission at around 655 nm (preferential chl b excitation at 475 nm). 77 K emission spectra of both proteoliposomes with and without MGDG reveal a very small 655 nm signal indicating that the vast majority of LHCII in proteoliposomes are intact (Fig. 2A), which is in agreement with the data in SI Fig. 2. Additionally, there is no difference in the 655 nm (F655) peak between MGDG containing and MGDG-depleted LHCII-proteoliposomes (see error bars in Fig. 2A). Furthermore, the emission around 700 nm (F700) is a signature for LHCII aggregation (33,40,41). F700 emission for detergent solubilized LHCII-trimers is about 10% relative to the maximal emission at around 681 nm (F681, 41). An increase in the F700/F681 ratio reflects LHCII-trimer aggregation. In LHCII-proteoliposomes the F700/F681 ratio is 15-16% (Fig. 2A). This low F700/F681 ratio in LHCII-proteoliposomes suggests a very low level of LHCII-trimer aggregation, as expected for highly protein diluted membranes. A low level of LHCII aggregation is also supported by fluorescence lifetime measurements (see below). As for the 655 nm emission, no statistically

significant difference of the F700/F681 ratio exists between proteoliposomes with and without MGDG (see error bars in Fig. 2A). These conclusions are supported and complemented by CD spectra of LHCII-proteoliposomes. The CD spectra in the Soret region show a pronounced negative peak at 472 nm ((-)472 nm) that is characteristic for trimeric LHCII and is absent in monomeric LHCII (42,43,44). In detail the (-)472nm to (-)490 nm ratio in trimeric LHCII is between 0.7 and 0.75 (43,44) that is very similar to the ratio of 0.72 in our LHCII-proteoliposomes (Fig. 2B). Further support for a trimeric LHCII organization in proteoliposomes is given by the broad (+)412 nm signal (Fig. 2B) that is absent in LHCII monomers (42). Clear signatures for LHCII aggregation are the occurrence of a (-)438 nm peak and a significant reduced (-)676 nm peak (45). Absence of these signatures in CD spectra of the LHCII-proteoliposomes (Fig. 2B) indicate that LHCII is in a non-aggregated state, which is in line with the low F700/F681 ratio (see above). There are also no significant differences in CD spectra in MGDG-containing and MGDG-depleted proteoliposomes. Overall, the fluorescence and CD spectra demonstrate the structural integrity of LHCII in our proteoliposomes and its organization as a non-aggregated trimer.

Impact of MGDG on the LHCII fluorescence yield. A straightforward method for detecting energy quenching in isolated LHCII is the measurement of the relative chl fluorescence yield (Φ_{fluor}) since a decrease in Φ_{fluor} gives strong indication for an increased dissipative deactivation of electronic excited states into heat. Φ_{fluor} of the various samples can be compared by normalizing the maximal fluorescence intensity by the absorbance of each sample at the excitation wavelength. This fluorescence to absorption ratio (Φ_{fluor}) quantifies the amount of light emitted from LHCII per light absorbed by the pigment protein complex. Excitations wavelengths probing either preferentially chl a (420 nm) or chl b (475 nm) were used (SI Fig 2). In order to determine the absorption values at 420 nm (Abs_{420}) and 475 nm (Abs_{475}) the spectra were baseline corrected for an unspecific light scattering background (continuous increase from red to blue spectral regions) caused by the proteoliposomes (SI Fig. 2E). Room temperature fluorescence excited at either 420 nm (SI Fig. 2A) or 475 nm (SI Fig. 2B) was measured from the same samples used for absorption spectroscopy allowing Φ_{fluor} calculation. To compare MGDG-containing and MGDG-depleted proteoliposomes the Φ_{fluor} for -MGDG proteoliposomes were set to one (Fig. 3). It turns out that Φ_{fluor} for LHCII in MGDG-containing proteoliposomes is about 25% lower compared to their MGDG-depleted counterparts. This result provides strong evidence that the presence of MGDG in lipid bilayers causes energy quenching in trimeric LHCII. To study the impact of MGDG on energy quenching in LHCII in more detail a third MGDG concentration was added at around 10 mol% MGDG (Fig. 3B). Φ_{fluor} in LHCII-proteoliposomes with about 10 mol% MGDG is very similar to Φ_{fluor} in MGDG-depleted samples.

Chl fluorescence lifetime analysis of LHCII proteoliposomes. A more in depth characterization of MGDG-dependent energy quenching in LHCII was performed by measuring chl fluorescence lifetimes in +MGDG and –MGDG proteoliposomes by time correlated single photon counting (TCSPC) (Fig. 4). Fig. 4A gives examples for chl fluorescence relaxation kinetics for +MGDG and -MGDG LHCII-proteoliposomes. Kinetics for +MGDG proteoliposomes are clearly faster than in MGDG-depleted samples, suggesting that

MGDG causes shortening of the excited state lifetime in LHCII. For both types of proteoliposomes the fluorescence relaxation kinetics can be fitted by bi-exponential decay curves as is typical for isolated trimeric LHCII (28,46,47,48). It was confirmed that the bi-exponential parameters derived from TCSPC analysis are independent on the laser power used for this experiment (SI Fig. 3) indicating absence of exciton-exciton annihilation events. The average fluorescence lifetime (τ_{av}) for MGDG-depleted proteoliposomes calculated from a bi-exponential fit is 3.66 ns (Fig. 4B). This lifetime is in agreement with literature values for non-aggregated trimeric LHCII in detergent shells that are around 3.6 ns (28,40,35,47). The good correlation of average fluorescence lifetimes between LHCII in detergent and LHCII in MGDG-depleted proteoliposomes indicates that LHCII is in a non-energy-quenched light-harvesting state in the latter. Closer inspection of the LHCII fluorescence kinetics in MGDG-depleted proteoliposomes reveal that the faster exponential component has a time constant of τ_{fast} = 0.46 ns with a relative amplitude (A) of A_{fast} = 0.15 (Fig. 4). For the slower dominating component (A_{slow} = 0.85) τ_{slow} is 4.24 ns. It is noteworthy that the τ_{fast} (~0.5 ns) component is most likely not caused by LHCII aggregation (48). Rather it was hypothesized that the slow and fast fluorescence lifetimes reflect two conformations of non-aggregated LHCII-trimers (48). No indication was found for a component with very long lifetimes that would indicate free chls, which have fluorescence lifetimes of around 6 ns (46,48,49). For example, chls that unbind from LHCII trimers by high Triton X-100 concentrations show lifetimes of about 5.8 ns (46,48). The absence of these very long living decay components supports the conclusions that LHCII in proteoliposomes is structurally intact (see above). Addition of ~25 mol% MGDG to LHCII proteoliposomes induces significant changes in all four bi-exponential fluorescence relaxation parameters (Figs. 4C and 4D). In detail, A_{fast} increases slightly by ~4% at the expense of A_{slow}. At the same time τ_{slow} (3.4 ns) is ~20% faster and τ_{fast} (0.63 ns) ~37% slower in MGDG-containing LHCII-proteoliposomes. As a consequence of these alterations in the two exponential fluorescence decay phases in +MGDG proteoliposomes the average lifetime (τ_{av}) of LHCII decreased by 17% (3.05 ns) relative to their –MGDG counterparts (Fig. 4B). If the decrease of the steady state chl fluorescence yield (Φ_{fluor}, Fig. 3A) is exclusively caused by shortening of fluorescence lifetimes (activation of energy dissipative pathways in LHCII) then it is expected that the MGDG-induced decrease in τ_{av} and the corresponding decreases in Φ_{fluor} have the same magnitude. The MGDG-induced decrease in Φ_{fluor} seems slightly higher with ~25%. However, it must be pointed out that this difference between τ_{av} and Φ_{fluor} is statistically not significant (see error bar in Fig. 3A). It follows that the decline in fluorescence yield of LHCII in +MGDG liposomes could be entirely explained by a shortening of fluorescence lifetimes.

Discussion

For non-photosynthetic membranes, there is good evidence that generic physicochemical properties of lipid bilayers modulated by non-bilayer lipids exert control over membrane protein conformation and function. Until today the role of the non-bilayer thylakoid lipid MGDG on photosynthetic light harvesting is unknown. This study employed proteoliposomes to study the role of MGDG on the structure and function of plant LHCII. The benefit of proteoliposomes is that they are compositionally and structurally well defined, i.e. they offer a significant advantage over complex structured intact thylakoid

membranes for identification of cause and effect relationships. A prerequisite to examine lipid-induced alterations on LHCII structure and function with proteoliposomes is avoidance of LHCII aggregation by a drastic dilution in protein density. To our knowledge, only two publications performed studies on LHCII on highly protein-diluted proteoliposomes. However, in both publications severe problems were reported for highly protein-diluted samples. In (30) LHCII-trimers monomerized and in (31) proteoliposomes without MGDG form mixtures of lipid vesicles and planar sheets making the direct comparison with their MGDG containing counterparts difficult. Here we established a LHCII-proteoliposome reconstitution protocol with very low protein densities (molar lipid/LHCII-trimer ratio ~60,000) embedded in large (~200 nm diameter) LUVs with different mol% of MGDG. The large proteoliposome diameter ensures minimized membrane bending forces for LHCII in the lipid bilayer. In detail, the curvature of a proteoliposome with 200 nm diameter leads to height difference of the lipid bilayer on two opposite sides of the LHCII trimer (distance 7.5 nm) of less than three Å, i.e. LHCII experience an almost flat lipid-membrane that resembles the situation in native thylakoid membranes. Steady state fluorescence, CD spectroscopic, and fluorescence lifetime analyses of LHCII for both MGDG-depleted and MGDG-containing proteoliposomes (Fig. 2) reveal the structural integrity of the complex (no chl unbinding) as well as its organization as a non-aggregated trimer, laying the foundation to study lipid-LHCII interactions specifically. The key outcome of this study is that presence of MGDG in proteoliposomes leads to significant energy quenching of LHCII (Φ_{fluor} is lower and τ_{av} is shorter, Figs. 3 and 4). Since nothing else changed in the two types of proteoliposomes except the MGDG content (i.e. both –MGDG and +MGDG proteoliposomes contain the same amount of charged lipids, Fig. 1D) this result gives strong evidence for the specific role of the non-bilayer MGDG for modulating light-harvesting by LHCII, i.e. MGDG in lipid bilayers induces energy quenching in LHCII. However, it is noteworthy that the MGDG-induced change in fluorescence lifetimes from 3.66 to 3.05 ns is a magnitude higher than the photochemical trapping time in PSII (300 to 500 ps), i.e. the impact on competing with photochemistry is small. On the other hand, we want to point out that native thylakoid membranes contain about ~50 mol% MGDG thus the fluorescence quenching observed here with ~20 mol% could be significant higher in native thylakoid membranes.

An intriguing question is the molecular mechanism of how non-bilayer MGDG determines the light-harvesting efficiency of LHCII. One possibility is that modulation of the LMP by MGDG leads to conformational changes in LHCII that trigger dissipative pathways for excited pigment states. To explore this possibility in more detail we generated an in-scale model of the LHCII-trimer together with LMP changes induced by MGDG derived from molecular dynamics simulations (25) (Fig. 5). Fig. 5 gives the false-color coded structural flexibility of LHCII that is derived from the crystallographic temperature (or B) factor (8). The color code varies from very rigid regions (blue) to highly flexible regions (red). As expected for a membrane integral protein complex the hydrophobic part made of rigid α-helices embedded in the lipid bilayer is mostly very stiff (8,50,51). However, an important exception is the xanthophyll neoxanthin (neo) that protrudes from the protein surface into the fatty acid region of the lipid bilayer. This neo is highly flexible (8,51). Comparing MGDG-induced lateral pressure changes along the z-axis of the lipid bilayer (red curve in Fig. 5, bottom) with the

LHCII flexibility reveals a significant (several 10 MPa) increase in lipid-bilayer pressure on the level of neo (orange arrow). Thus, it is likely that the presence of MGDG in lipid bilayers leads to bending of LHCII-bound neo as was reported for LHCII crystals where adjacent LHCII proteins cause neo bending (34). Interestingly, based on the fact that neo distortion correlates with energy dissipation (51,52,53) it was hypothesized that the bending of LHCII-bound neo switches the protein from a light-harvester to an energy dissipator (52,54). Indeed, molecular dynamics simulation identified a strong correlation between neo bending, pigment rearrangement in LHCII, and energy quenching (51). However, it is also possible that neo distortion is not the trigger but only a reporter for an energy dissipative state that is established by other pigment-pigment rearrangements (e.g. Chl a603-lutein2) (51). Also, chls a611/612 are potential candidates for LMP – induced quenching since they are localized at the LHCII periphery (pdb #1RWT). We speculate that the lateral pressure increase at a certain z-position in the lipid bilayer, caused by MGDG, leads to distortion of neo or other pigment-pigment rearrangements and switches LHCII to an energy quenching state (Fig. 5, bottom). A direct impact of physical pressure on light harvesting by LHCII was observed by studying the functionality of the isolated detergent-solubilized protein at different isotropic hydrostatic pressures measured with a high-pressure cell (48). In accordance with our study τ_{av} and Φ_{fluor} decrease with an increase in hydrostatic pressure in the pressure cell, i.e. LHCII switches to an energy quenched mode (48). The similarities in both studies goes further: In (48) the amplitudes of the two fluorescence lifetime components change with increasing pressure, i.e. A_{slow}/A_{fast} decreases. The same tendency is observed for +MGDG liposomes. A_{slow}/A_{fast} decreases from 5.6 in MGDG-depleted proteoliposomes to 4.4 in MGDG-containing samples (Fig. 4C). Furthermore, in the isotropic pressure cell experiment τ_{slow} accelerates whereas τ_{fast} decelerates with higher pressure (48). We observed the same changes from –MGDG to +MGDG proteoliposomes (Fig. 4D). These similarities between isotropic hydrostatic pressure experiments on detergent-solubilized LHCII trimers and the impact of MGDG in LHCII-proteoliposomes supports the model that the MGDG-dependent pressure increases in hydrophobic regions of the lipid bilayer are sensed by flexible LHCII parts leading to energy quenching (Fig. 5). An intriguing outcome of the study of (48) is that pressure-induced energy quenching is caused by very localized and small conformational changes and not by large scale compression of the overall protein. These localized structural changes explicitly include the possibility of neo bending (48) in support of our model presented in Fig. 5.

The physiological relevance for a LMP-dependent mechanism to switch LHCII structure and function as proposed here is given if the LMP is variable, i.e. the LMP can be changed by environmental factors. Three observations indeed indicate that LMP in thylakoid is variable. (i) Under certain conditions MGDG separates to non-bilayer HII phases in intact thylakoid membranes (e.g. 55,56,57,58). This lipid phase separation of MGDG would decrease the abundance of MGDG in the bilayer phase. As a consequence, the lateral membrane pressure in hydrophobic membrane bilayer regions decreases that according to the model in Fig. 5 would switch LHCII to a light-harvesting state. Interestingly HII formation was found stimulated by low light treatment (58), i.e. at situations where efficient light harvesting is required and not photoprotection. (ii) The results summarized in (i) measured large-scale HII formation that are visible in electron micrographs. However,

recent molecular dynamics simulations indicated that non-bilayer HII formation could be more frequent on a smaller nanometer length scale that is not detectable by conventional electron microscopy (36) as was proposed earlier (56). The molecular dynamics study reveals that the propensity for HII formation is strongly dependent on environmental conditions (e.g. water content). (iii) The LMP profile is a generic physicochemical property of the lipid bilayer and is therefore dependent not only on non-bilayer lipids but on all lipophilic membrane components. In this respect, the xanthophyll zeaxanthin (zea) is interesting. The presence of zea in the lipid bilayer increases membrane order and rigidity (59,60) that is known to enhance the lateral membrane pressure in hydrophobic membrane regions (13). Zea is converted from violaxanthin by the xanthophyll cycle and promotes qE formation (61,62). Thus, modulation of generic physicochemical membrane properties by free zea in the membrane could be another way to control LMP and therefore light harvesting by LHCII. It follows that the xanthophyll cycle has two implications. First, zea would activate qE directly by the well-established binding to LHCIIs (61). Second, zea could modulate light harvesting indirectly via changes in LMP. The three examples presented above demonstrate that the lipid matrix in thylakoid membranes is dynamic and responsive to environmental conditions that could modulate the LMP that in turn could control light harvesting efficiency by LHCII (Fig 5). Furthermore, evidence exist that the lipid/fatty acid content in plant thylakoid membranes undergo diurnal alterations (63, 64) and change under stress like heat (65), cold (66), hypoxia (67), drought (68), and phosphate starvation (69). However, future studies have to reveal the dynamics of lipid/fatty acid compositions and its implications on light harvesting.

Experimental Procedure

Isolation of trimeric LHCII. Trimeric LHCII was isolated from dark-adapted spinach from local market according to (41). This protocol goes back to the original Triton-X-100 based isolation procedure described in (70,71). The final LHCII preparation was solubilized in 0.37% Triton X-100 at a chl concentration of 1.65 mM.

Preparation of LHCII proteoliposomes: For liposomes the isolated plant lipids MGDG (C36:6 and C34:6), DGDG (C36:6 and C34:3), PG (C34:4 and C34:3) SQDG (C34:3) were used (Lipid Products, UK). Approximately 5 μmol of isolated lipids in chloroform were mixed and evaporated off by nitrogen gas to form a thin lipid layer. The lipid film was rehydrated in a 10 mM HEPES buffer (pH 7.6, KOH) and vortexed thoroughly. The resulting multilamellar liposomes were passed sequentially through a 0.4 μm and 0.2 μm nucleopore membrane using a high-pressure extruder (Lipex™) at approximately 3.5 bar for the 0.4 μm extrusion, and 10 bar for the 0.2 μm extrusion, leading to large unilamellar vesicles (LUVs). The lipid concentration in LUVs was determined by 2D thin layer chromatography (TLC) as described in (71). The lipid concentration in LUV stock was adjusted to 0.8 mM in 1.6 mL. Triton X-100 was added to a final concentration of 1 mM to destabilize the liposomes. After 5 minutes of incubation under slow stirring, 200 μL of isolated LHCII at a chl concentration of 25 μM (presolubilized in 600 μM Triton X-100/10 mM HEPES, pH 7.6) was added and incubated for 30 minutes at room temperature (incorporation of the protein into LUVs), the Triton X-100 was removed with 25 mg Bio-beads™ SM-2 Resin overnight at 4 C, followed by two 100 mg Bio-beads™ addition steps for an hour, and 45 minutes, respectively. The Triton removal was tracked using the 275 nm absorbance. Finally,

proteoliposomes were further purified by gel filtration with a PD-10 Sephadex filtration column. Proteoliposomes were stored on ice in the dark and used freshly. The pigment composition of proteoliposomes with and without MGDG are (relative to total Chl): neoxanthin, 0.9±0.1 and 1.0±0.1; violaxanthin, 0.2±0.1 and 0.3±0.1; lutein 2.4±0.1 and 2.3±0.1, respectively. No zeaxanthin was detected.

Biochemical characterization. The lipid classes (MGDG, DGDG SQDG, PG) of proteoliposomes were quantified from lipid extracts by 2D thin layer chromatography (73). From the same lipid extract fatty acids were converted to fatty acid methyl esters (FAME) and quantified with gas chromatography (GC) by comparison of the fatty acid GC peaks with an internal fatty acid standard (2.613 nmol μl^{-1} 1,2,3-tripentadecanoyl-sn-glycerol, Nu-Chek Prep) as described in (65).

Steady state fluorescence spectroscopy. For Φ_{fluor} measurements anaerobic conditions with undiluted proteoliposomes (OD420nm = 0.1) were established with a glucose/glucose-oxidase/catalase system. Oxygen measurements with a polarography oxygen electrode reveal anaerobiosis after about one minute with this enzyme system for about one hour. Anaerobiosis was required to minimize damage to LHCII due to the measuring lights (the lack of damage was indicated by unchanged signal amplitudes in repetitive measured fluorescence spectra). The same anaerobic sample was used for both absorption and fluorescence spectra to determine Abs_{420} and Abs_{475} and the maximum fluorescence intensities at these excitation wavelengths. Optical absorption spectra were recorded with a Hitachi U3900 spectrometer (2-nm slit width, 200-750 nm, optical path length 10 mm). Chl fluorescence spectra were measured with a FluoroMax 4 (Horiba Yvon) spectrofluorometer. Emission spectra between 640 to 800 nm (slit width 4 nm) were recorded for 420 or 475 nm excitation wavelength (slit width 2 nm). Fluorescence spectra at 77 K were measured with samples shock-frozen in liquid nitrogen. The excitation wavelength was set to 475 nm (2 nm slit width).

CD Spectroscopy. VIS-CD (circular dichroism between 400 to 700 nm) spectroscopy measurements were performed with an AVIV 202SF CD spectrometer in a 0.5 cm cuvette in 10 mM HEPES/KOH buffer with concentrated proteoliposomes. The proteoliposomes concentration was performed with Amicon Ultra (30 kDa exclusion size). Re-dilution of concentrated proteoliposomes leads to not alteration in 77 K fluorescence spectra indicating that the concentration did not changed LHCII integrity. Spectra recorded with HEPES buffer alone were subtracted. Measurements were done under anaerobic conditions (glucose/glucose-oxidase/catalase system).

Time correlated single photon counting (TCSPC). Time correlated single photon counting (TCSPC) measurements of fluorescence lifetime were acquired using Becker-Hickl module SPC-150 in conjunction with Becker-Hickl SPCM software. The 420 nm excitation pulses with a repetition rate of 3.8 MHz were generated by a Coherent Verdi G10 532 nm diode pumped laser which pumps a Coherent Mira 900f Ti:Sapphire Oscillator set to 840 nm. The resultant pulsed beam was then frequency doubled using a β-barium borate (BBO) crystal to obtain 420 nm pulses at a repetition rate of 76 MHz. A pulse picker composed of a Harris SiO_2 crystal, and a Coherent 7200 cavity dumper in combination with an ENI voltage amplifier (model 403LA) to drive the acoustic waves was used

to reduce the repetition rate to the desired 3.8 MHz for these experiments. Samples were prepared to have an optical density of approximately 0.1 and measured in a Starna cell cuvette at room temperature with Spectrosil far UV Quartz windows, a 1 mm path-length (front face detection) and a 0.4 mL volume. In order to obtain sufficient fluorescence counts from the sample, a long pass filter (polarizer set to magic angle) was used to detect wavelengths longer than 650 nm. 420 nm light was used to excite the chlorophyll a Soret band. Fluorescence was detected using a Hamamatsu R3809U microchannel plate photomultiplier tube (MCP PMT) and the IRF had a full width half max of approximately 60 ps. Measurements were taken at several powers and it was determined that there was no power dependence for measurements taken at average powers less than 100 μW (SI Fig. 3). Therefore, all measurements taken at powers below 100 μW were averaged to obtain a larger sample size. The full width at half maximum of the laser spot was about 650 μm. Under our conditions the fluorescence lifetimes were unchanged for at least 60 min indicating stability of the samples over the time of measurements.

Dynamic light scattering. The diameter of the LUVs and proteoliposomes was measured in a 10 mm cuvette using a Delsa™ Nano Zeta Potential and submicron particle size analyzer (Beckmann-coulter). Latex beads (Beckman-coulter) between 100 nm and 300 nm in diameter were used to create a size standard curve. The liposome and proteoliposome diameters were determined from this standard curve.

Acknowledgement

This research was supported by the National Science Foundation (MCB-1616982) the US Department of Energy (DE-SC 0017160), and USDA National Institute of Food and Agriculture Hatch projects #1005351 and #0119 (all H.K.). This work was also supported by the Director, Office of Science, Office of Basic Energy Sciences, of the US Department of Energy under Contract DE-AC02-05CH11231 and the Division of Chemical Sciences, Geosciences, and Biosciences, Office of Basic Energy Sciences of the US Department of Energy through Grants DE-AC03-76SF000098 and FWP 449B (all G.R.F). We wish to thank Bart van Oort for help with TCSPC measurements and for many fruitful discussions.

Conflict of interests

The authors declare no conflict interests.

References

1. Mirkovic T, Ostroumov EE, Anna JM, van Grondelle R, Govindjee, Scholes GD (2017) Light absorption and energy transfer in the antenna complexes of photosynthetic organisms. *Chem Rev.* 117: 249-293.
2. Croce R, van Amerongen H (2014) Natural strategies for photosynthetic light harvesting. *Nat Chem Biol.* 10: 492-501.
3. Krüger T, Wientjes E, Croce R, van Grondelle R (2011) Conformational switching explains the intrinsic multifunctionality of plant light-harvesting complexes. *Proc. Natl. Acad. Sci USA* 108: 13516-13521.

4. Niyogi KK, Truong TB (2013) Evolution of flexible non-photochemical quenching mechanisms that regulate light harvesting in oxygenic photosynthesis. *Curr Opin Plant Biol.* 16: 307-314.
5. Ruban AV (2016) Nonphotochemical chlorophyll fluorescence quenching: mechanism and effectiveness in protecting plants form photodamage. *Plant Physiol* 170: 1903-1916.
6. Kuehlheim C, Agren J, Jansson S (2002) Rapid regulation of light harvesting and plant fitness in the field. *Science* 297: 91-93.
7. Liu Z, Yan H, Wang K, Kuang T, Zhang J, Gui L, An X, Chang W (2004) Crystal structure of spinach major light-harvesting complex at 2.72-Å resolution. *Nature* 428: 287–292.
8. Barros T, Royant A, Standfuss J, Dreuw A, Kühlbrandt W (2009) Crystal structure of plant light-harvesting complex shows the active, energy-transmitting state. *EMBO J.* 28: 298-306.
9. Müh F, Madjet Mel-A, Renger T. (2010) Structure-based identification of energy sinks in plant light-harvesting complex II. *J Phys Chem B*. 114: 13517-13535.
10. Novoderezhkin V, Marin A, van Grondelle R (2011) Intra- and inter-monomeric transfers in the light harvesting LHCII complex: the Redfield-Förster picture. *Phys Chem Chem Phys* 13: 17093-17103.
11. Chmeliov J, Gelzinis A, Songaila E, Augulis R, Duffy CD, Ruban AV, Valkunas L (2016) The nature of self-regulation in photosynthetic light-harvesting antenna. *Nat Plants* 18: 16045.
12. Cantor RS (1997) Lateral pressure profiles in cell membranes: A mechanism for modulation of protein function. *J. Phys. Chem. B* 101: 1723-1725
13. Gullingsrud J, Schulten K (2004) Lipid bilayer pressure profiles and mechanosensitive channel gating. *Biophys. J.* 86: 3496-3500
14. Karasawa A, Swier LJ, Stuart MC, Brouwers J, Helms B, Poolman B (2013) Physicochemical factors controlling the activity and energy coupling of an ionic strength-gated ABC transporter. *J. Biol. Chem.* 288: 29862-29871
15. Philipps R, Ursell T, Wiggins P, Sens P (2009) Emerging roles for lipids in shaping membrane-protein function. *Nature* 459: 379-385
16. Khalili-Araghi F, Gumbart J, Wen P-C, Sotomayor M, Tajkhorshid E, Schulten K (2009) Molecular dynamics simulations of membrane channels and transporters. *Curr. Opin. Struct. Biol.* 19: 128-137.
17. Anishkin A, Loukin SH, Teng J, Kung C (2014) Feeling the hidden mechanical forces in lipid bilayer is an original sense. Proc Natl Acad Sci USA 111: 7898-7905.
18. van den Brinck-van den Laan E, Kilian JA, de Kruijff B (2004) Nonbilayer lipids affect peripheral and integral membrane proteins via changes in the lateral pressure profile. *Biochim Biophys Acta* 1666: 275-288.
19. Israelachvili JN, Marcelja S, Horn RG (1980) Physical principles of membrane organization, *Q. Rev. Biophys*. 13: 121-200.
20. Boudière L, Michaud M, Petroutsos D, Rébeillé F, Falconet D, Bastien O, Roy S, Finazzi G, Rolland N, Jouhet J, Block MA, Maréchal E (2014) Glycerolipids in photosynthesis: composition, synthesis and trafficking. Biochim Biophys Acta. 1837: 470-480.
21. Garab G, Ughy B, Goss R. (2016) Role of MGDG and Non-bilayer lipid phases in the structure and dynamics of chloroplast thylakoid membranes. *Subcell Biochem.* 86: 127-157.
22. Seiwert D, Witt H, Janshoff A, Paulsen H (2017) The non-bilayer lipid MGDG stabilizes the major light-harvesting comoplex (LHCII) against unfolding. Sci Rep 7: 5158.

23. Orsi M, Essex JW (2013) Physical properties of mixed bilayers containing lamellar and nonlamellar lipids: insights from coarse-grain molecular dynamics simulations. *Faraday Discuss.* 161: 249-272.
24. De Kruijff B (1997) Lipids beyond the bilayer. *Nature* 386: 129-130.
25. Baczynski K, Markiewicz M, Pasenkiewicz-Gierula M (2015) A computer model of a polyunsaturated monogalactolipid bilayer. *Biochimie* 118: 129-140.
26. Rigaud JL, Pitard B, Levy D (1995) Reconstitution of membrane proteins into liposomes: application to energy-transducing membrane proteins. *Biochim. Biophys. Acta* 1231: 223-246.
27. McDonnel A, Staehelin LA (1980) Adhesion between liposomes mediated by the chlorophyll a/b light-harvesting complex isolated from chloroplast membranes. *J Cell Biol.* 84: 40-56.
28. Moya I, Silvestri M, Vallon O, Cinque G, Bassi R (2001) Time-resolved fluorescence analysis of the photosystem II antenna proteins in detergent micelles and liposomes. *Biochemistry* 40: 12552-12661.
29. Yang C, Boggasch S, Haase W, Paulsen H (2006) Thermal stability of trimeric light-harvesting chlorophyll a/b (LHCIIb) in liposomes of thylakoid lipids. *Biochim Biophys Acta* 1757: 1642-1648.
30. Natali A, Gruber JM, Dietzel L, Stuart MCA, van Grondelle R, Croce R (2016) Light-harvesting complexes (LHCs) cluster spontaneously in membrane environment leading to shortening of their excited state lifetimes. *J Bio Chem* 291: 16730-16739.
31. Crisafi E, Pandit A (2017) Disteangling protein and lipid interactions that control a molecular switch in photosynthetic light harvesting. *Biochm Biophys Acta* 1859: 40-47.
32. Rigaud JL, Levy D (2003) Reconstitution of membrane proteins into liposomes. *Methods Enzymol.* 372: 65-86.
33. Horton P Ruban AV, Rees D, Pascal AA, Noctor G, Young AJ (1991) Control of the light-harvesting function of chloroplast membranes by aggregation of the LHCII chlorophyll-protein complex. FEBS Lett 292, 1-4
34. Pascal AA, Liu Z, Broess K, van Oort B, van Amerongen H, Wang C, Horton P, Robert B, Chang W, Ruban A (2005) Molecular basis of photoprotection and control of photosynthetic light-harvesting. *Nature* 436: 134-137.
35. Akhtar P, Dorogi M, Pawlak K, Kovács L, Bóta A, Kiss T, Garab G, Lambrev PH (2015) Pigment interactions in light-harvesting complex II in different molecular environments. *J. Biol Chem* 290: 4877-4886.
36. Van Eerden FJ, de Jong DH, de Vries AH, Wassenaar TA, Marrink SJ (2015) Characterization of thylakoid lipid membranes from cyanobacteria and higher plants by molecular dynamics simulation. *Biochim Biophys Acta* 1848: 1319-1330.
37. Joyard J, Marechal E, Miege C, Block MA (1998) Structure, distribution and biosynthesis of glycerolipids from higher plant chloroplasts. In: Lipids in photosynthesis: structure function and genetics (Siegenthaler PA, Murata N, eds), Kluwer Academic Publishers, The Netherlands: 21-52.
38. Sprague SG, Staehelin A (1984) Effects of reconstitution method on the structural organization of isolated chloroplast membrane lipids. *Biochim Biophys Acta* 777: 306-322.
39. Croce R, Cinque G, Holzwarth AR, Bassi R (2000) The Soret absorption properties of carotenoids and chlorophylls in antenna complexes of higher plants. *Photosyn Res* 64: 221-231.

40. Pandit A, Shirzad-Wasei N, Wlodarczyk LM, van Roon H, Boekema EJ, Dekker JP, de Grip WJ (2011) Assembly of the major light-harvesting complex II in lipid nanodiscs. *Biophys. J.* 101: 2507-2515.
41. Kirchhoff H., Hinz HJ, Rösgen J (2003) Aggregation and fluorescence quenching of chlorophyll a of the light-harvesting comples II from spinach in vitro. Biochim Biophys Acta 1606, 105-116
42. Hobe S, Prytulla S, Kühlbrandt W, Paulsen H (1994) Trimerization and crystallization of reconstituted light-harvesting chlorophyll a/b complex. *EMBO J* 13: 3423-3429.
43. Georgakopoulou S, van der Zwan G, Bassi R, van Grondelle R, van Amerongen H, (2007) Understanding the changes in the circular dichroism of light harvesting complex II upon varying its pigment composition and organization. *Biochem.* 46: 4745-4754.
44. Yang C, Lambrev P, Chen Z, Jarvorfi T, Kiss AZ, Paulsen H, Garab G (2008) The negatively charged amino acids in the lumenal loop influence the pigment binding and conformation of the major light-harvesting chlorophyll a/b complex of photosystem II. *Biochim. Biophys. Acta* 1777: 1463-1470.
45. Ruban AV, Calkoen F, Kwa SLS, Grondelle R van, Horton P, Dekker JP (1997) Characterisation of LHC II in the aggregated state by linear and circular dichroism spectroscopy. *Biochim. Biophys. Acta* 1321: 61-70.
46. Ide JP, Klug DR, Kühlbrandt W, Giorgi LB, Porter G (1987) The state of detergent solubilized light-harvesting chlorophyll-a/b protein complex as monitored by picosecond time-resolved fluorescence and circular dichroism. *Biochim Biophys Acta* 893: 349-364.
47. Palacios M, Standfuss J, Vengris M, van Oort BF, van Stokkum IH, Kühlbrandt W, van Amerongen H, van Grondelle R (2006) A comparison of the three isoforms of the light harvesting complex II using transient absorption and time-resolved fluorescence measurements. *Photosyn Res*. 88: 269-285.
48. van Oort B, van Hoek A, Ruban AV, van Amerongen H (2007) Equilibrium between quenched and nonquenched conformations of the major plant light-harvesting complex studied with high-pressure time-resolved fluorescence. *J Phys Chem B* 111: 7631-7637.
49. Palacios M, Frank L. de Weerd, Janne A. Ihalainen, van Grondelle R, van Amerongen H (2002) Superradiance and exciton (de)localization in light-harvesting complex II from green plants? *J Phys Chem B* 106: 5782-5787.
50. Dockter C, Müller AH, Dietz C, Volkov A, Polyhach Y, Jeschke G, Paulsen H. (2012) Rigid core and flexible terminus. *J Biol Chem* 287: 2915-2925.
51. Liguori N, Periole X, Marrink SJ, Croce R (2015) From light-harvesting to photoprotection: structural basis of the dynamic switch of the major antenna complex of plants (LHCII). *Sci. Rep.* 5: 15661.
52. Ruban, Berera R, Ilioaia C, van Stokkum IH, Kennis JT, Pascal AA, van Amerongen H, Robert B, Horton P, van Grondelle R (2007) Identification of a mechanism of photoprotective energy dissipation in higher plants. *Nature* 450: 575-578.
53. Haferkamp S, Haase W, Pascal AA, van Amerongen H, Kirchhoff H (2010) Efficient light-harvesting by photosystem II requires an optimized protein packing density in grana thylakoids. *J Biol Chem* 285: 17020-17028.
54. Ruban AV, Johnson MP, Duffy CDP (2012) The photoprotective molecular switch in the photosystem II antenna. *Biochim Biophys Acta* 1817: 167-181.
55. Webb MS, Green BR (1991) Biochemical and biophysical properties of thylakoid acyl lipids. *Biochim. Biophys. Acta* 1060: 133-158.

56. Garab G, Lohner K, Laggner P, Farkas T (2000) Self-regulation of the lipid content of membranes by non-bilayer lipids: a hypothesis. *Trends Plant Sci* 5: 489-494.
57. Krumova SB, Dijkema C, de Waard P, Van As H, Garab G, van Amerongen H (2008) Phase behaviour of phosphatidylglycerol in spinach thylakoid membranes as revealed by 31P-NMR. *Biochim Biophys Acta* 1778: 997-1003.
58. Kirchhoff H, Haase W, Wegner S, Danielsson R, Ackermann R, Albertsson PA (2007) Low-light-induced formation of semicrystalline photosystem II arrays in higher plant chloroplasts. *Biochem* 46: 11169-11176.
59. Gruszecki WI, Strzalka K (2005) Carotenoids as modulators of lipid membrane physical properties. *Biochim. Biophys. Acta* 1740: 108-115.
60. Chegeni FA, Perin G, Gupta KBSS, Simionato D, Morosinotto T, Pandit A (2016) Protein and lipid dynamics in photosynthetic membranes investigated by in-situ solid-state NMR. *Biochim Biophys Acta* 1857: 1849-1859.
61. Jahns P, Latowski D, Strzalka K (2009) Mechanism and regulation of the violaxanthin cycle: the role of antenna proteins and membrane lipids. *Biochim. Biophys. Acta* 1787: 3-14.
62. Park S, Fischer AL, Steen CJ, Iwai M, Morris JM, Walla PJ, Niyogi KK, Fleming GR (2018) Chlorophyll-carotenoid excitation energy transfer in high-light-exposed thylakoid membranes investigated by snapshot transient absorption spectroscopy. *J. Am. Soc.* 140: 11965-11973.
63. Browse J, Roughan PG, Slack CR (1981) Light control of fatty acid synthesis and diurnal fluctuations of fatty acid composition n leaves. *Biochem. J.* 196: 347-354.
64. Maatta S, Scheu B, Roth MR, Tamura P, Li M, Williams TD, Wang X, Welti R (2012)Levels of *Arabidopsis thaliana* leaf phosphatidic acids, phosphatidylserines, and most trienoate-containing polar lipid molecular species increase during the dark period of the diurnal cycle. *Frontiers Plant Sci*. 3: 49.
65. Chen J, Burke JJ, Xin Z, Xu C, Velten J (2006) Characterization of the Arabidopsis thermosensitive mutant atts02 reveals important role of galactolipids in thermotolerance. *Plant Cell Environ*. 29, 1437-1448.
66. Mollering ER Muthan B, Benning C (2010) Freezing tolerance in plants requires lipid remodeling at the outer chloroplast membrane. *Science* 330: 226-228.
67. Klecker M, Gasch P, Peisker H, Dörmann P, Schlicke H, Grimm B, Mustroph A (2014) A shoot-specific hypoxic response of Arabidopsis sheds light on the role of the phosphate-responsive transcription factor PHOSPHATE STARVATION RESPONSE 1. Plant Physiol. 165: 774-790.
68. Gasulla F, vom Dorp K, Dombrink I, Zähringer U, Gissch N, Dörmann P, Bartels D (2013) The role of lipid metabolism in the acquisaton of desiccaton tolerance in Craterostigma Plantagineum: a comparative approach. *Plant J.* 75: 726-741.
69. Härtel H, Dörmann P, Benning C. (2000) DGD1-independent biosynthesis of extraplastidic galactolipids after phosphate deprivation in Arabidopsis. *Proc. Natl. Acad. Sci. USA* 97, 10649-10654.
70. Burke JJ, Ditto CL, Arntzen CJ (1978) Involvement of the light-harvesting complex in cation regulation of excitation energy distribution in chloroplasts. *Arch Biochem Biophys* 187: 252–263.
71. Kühlbrandt W, Thaler T, Wehrli E (1983) The structure of membrane crystals of the light-harvesting chlorophyll *a*/*b* protein complex. *J Cell Biol* 96: 1414–142.
72. Haferkamp S, Kirchhoff H (2008) Significance of molecular crowding in grana membranes of higher plants for light harvesting by photosystem II. *Photosyn Res* 95: 129-134.

73. Kirchhoff H, Yarbrough R (2017) Evaluation of lipids for the study of photosynthetic membranes. *Methods Mol Biol* 1770: 305-316.

Figure Legends

Fig. 1. Establishing a LHCII-proteoliposome system. (**A**) Scheme of producing LHCII-proteoliposomes from LUVs by the detergent-mediated incorporation approach (see text for details). Graphs at the bottom shows absorption spectra at the different preparation steps. Note the Triton X-100 peak at 275 nm that disappears after Bio-bead treatment. (**B**) Proteoliposomes size determination by dynamic light scattering. The "+/-" gives half of full width at half maximum (N=5, biological repetitions). No difference was apparent between +MGDG and –MGDG proteoliposomes. (**C**) Molar lipid to trimeric LHCII ratio in proteoliposomes. Lipid content was determined from 2D-TLC, LHCII-trimer content from chl determination assuming 42 chls per trimer. Error bars represent 95% confidence interval (N=5, biological repetitions). (**D**) Lipid and fatty acid analysis. Upper panel shows the mol% for the four different lipid classes in +MGDG and –MGDG proteoliposomes measured by 2D-TLC. Error bars represent SD (N=3, biological repetitions for both +MGDG and –MGDG samples). Fatty acids for the individual lipid classes separated by TLC were quantified by GC. Error bars represent SD (N=4 for +MGDG and N=3 for –MGDG proteoliposomes).

Fig. 2. Spectroscopic characterization of LHCII-proteoliposomes. (**A**) Representative chl fluorescence spectra of +MGDG and –MGDG proteoliposomes. Note the low emissions at 655 nm (indicative for chl b) and 700 nm (indicative for LHCII aggregates). Error bars at both wavelengths represent SD from 13 biological repetitions. (**B**) Room-temperature CD spectra. The spectra show the mean of two biological replicates per sample type. A CD spectrum for the pure buffer was subtracted. Characteristic wavelength for LHCII-trimer and protein aggregation are indicated (see in the text for details).

Fig. 3. Quantum yields in fluorescence emission (Φ_{fluor}). (**A**) Comparison of Φ_{fluor} for +MGDG and –MGDG proteoliposomes measured for 475 nm and 420 nm excitation (indicated). The data were measured on pairs of +MGDG and –MGDG proteoliposomes prepared at the same day. Φ_{fluor} for +MGDG was normalized to the same day -MGDG counterpart (set to one). Data are from 11 pairs. Error bars represent SD and *** indicates p value of <0.001 (students t-test). The mol% of the +MGDG samples is about 20%. (**B**) Dependency of mol% MGDG in proteoliposomes on Φ_{fluor}. The mol% of MGDG was determined by TLC.

Fig. 4. Time correlated single photon counting (TCSPC) of chl fluorescence on LHCII proteoliposomes. (**A**) Representative examples of fluorescence relaxation kinetics after laser excitation (flash). (**B**) Relaxation kinetics were fitted with two exponentials. The average fluoresce lifetime τ_{av} was calculated from the amplitude-weighted single exponential lifetimes. (**C, D**) Amplitudes (**C**) and lifetimes (**D**) for the slow and fast fluorescence relaxation components. Error bars represent SD (N=7 for +MGDG and N=10 for -MGDG proteoliposomes). *** indicates p value of <0.001 (students t-test).

Fig. 5. In scale model of the LMP profile and the LHCII trimer structure for membranes with only bilayer forming lipids (**A**, DOPC) and membranes with non-bilayer MGDG (**B**). The LMP

profiles were taken from (25). The temperature-factor representation of the LHCII-trimer structure is from (8) and is a measure of the flexibility of the protein (blue, rigid; red, flexible). The position of neo (**A**) and the MGDG-induced increase in pressure in the fatty acid region (**B**, orange arrow) are indicated. See the text for additional details.

Fig. 1

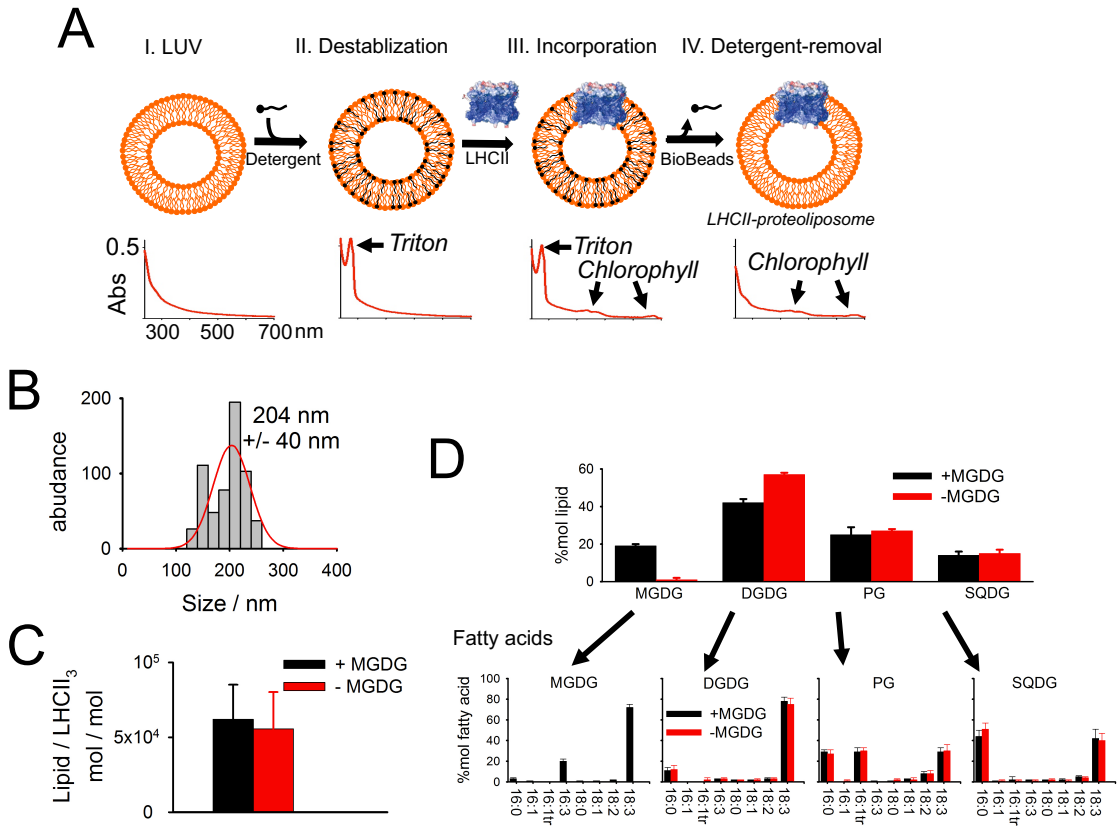

Fig. 2

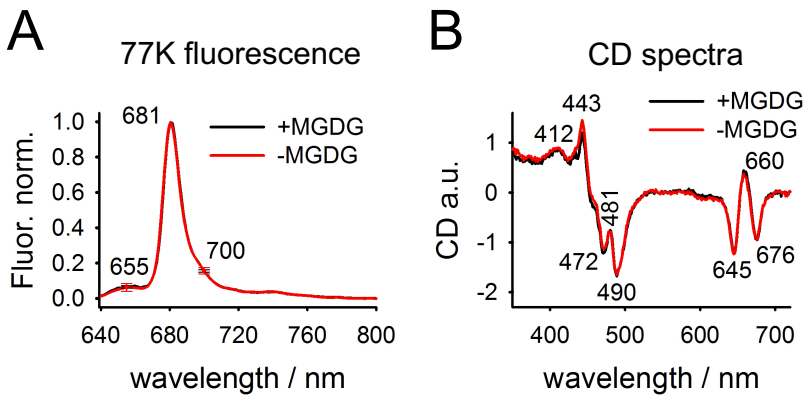

Fig. 3

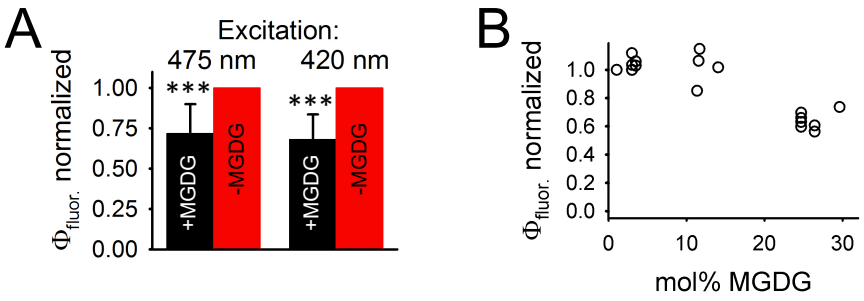

Fig. 4

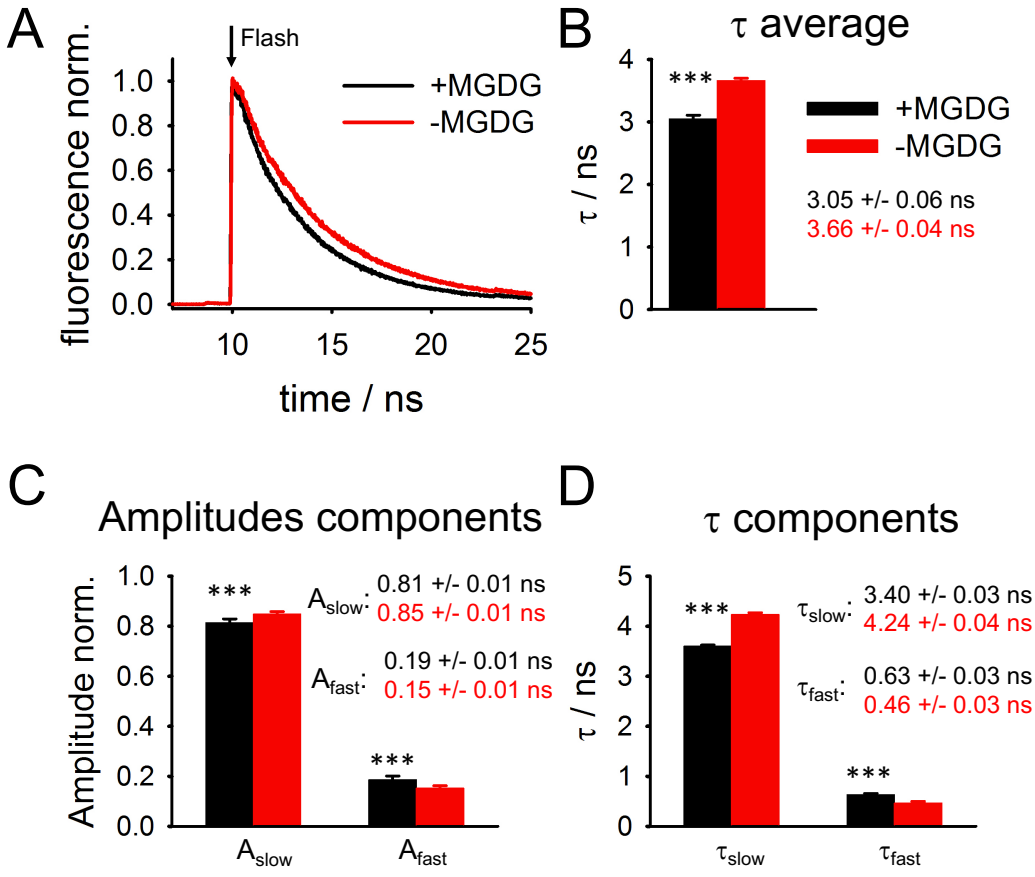

Fig. 5

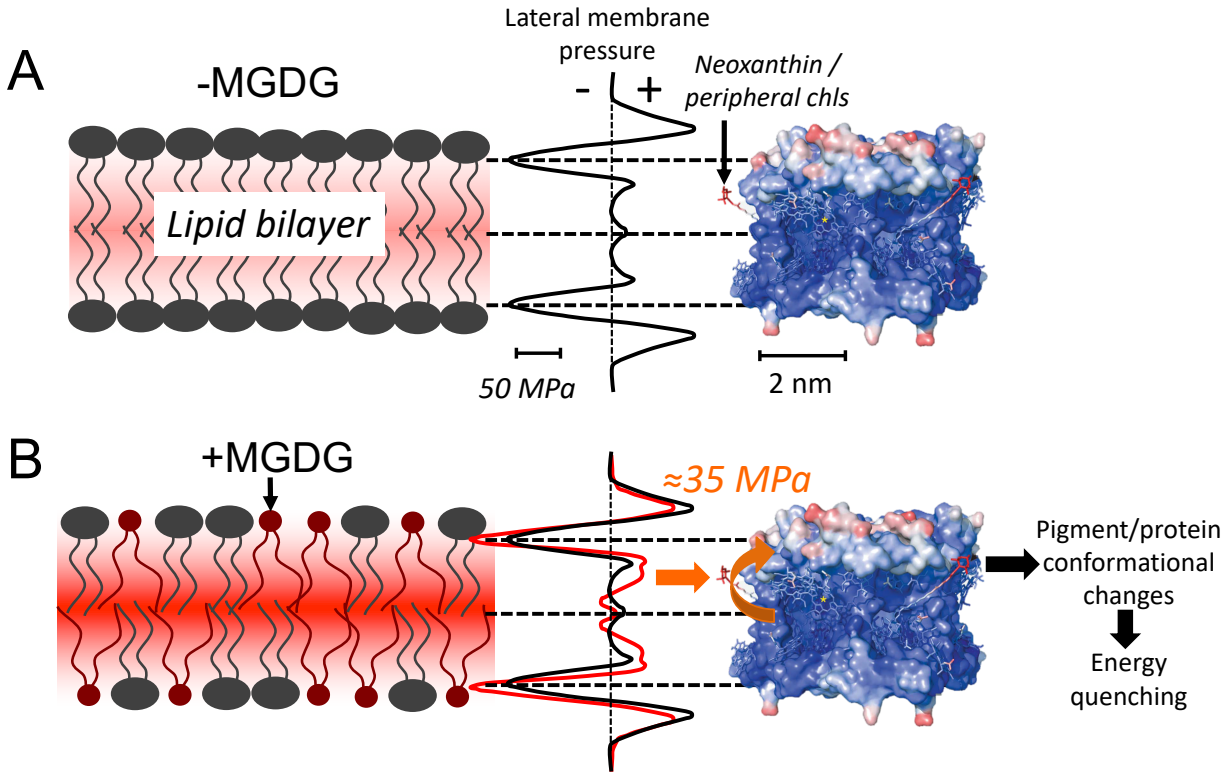
A
-MGDG
Lateral membrane pressure
-
+
Neoxanthin / peripheral chls
Lipid bilayer
50 MPa
2 nm
B
+MGDG
≈35 MPa
Pigment/protein conformational changes
Energy quenching

A proteoliposome-based system reveals how lipids control photosynthetic light harvesting

Stefanie Tietz, Michelle Leuenberger, Ricarda Höhner, Alice H Olson, Graham R Fleming and Helmut Kirchhoff

J. Biol. Chem. published online January 12, 2020
